Chapter 3
Improved Substructure Identification Through Use of an Active Control Device

Charles DeVore, Erik A. Johnson, and Richard E. Christenson

Abstract Increasingly, researchers turn to substructure identification for civil structural health monitoring for a variety of reasons. First, substructure identification provides inherent damage localization. Second, substructure identification provides greater numerical conditioning than full structure identification because only a small subset of the degrees of freedom are considered in each analysis. Third, substructure identification is perfectly suited for a decentralized implementation within a network of wireless sensors. This implementation can realize cost savings in installation and operation.

While the benefits of substructure identification are many-fold, current research shows that certain structure-substructure combinations admit poor performance. Research demonstrates that single story substructures in a shear building are poorly identified (if at all) when interstory acceleration response is low in a specific frequency range. This result shows that portions of the structure are unable to be identified properly with substructure identification.

To overcome these results, this paper temporarily re-purposes a structural control device to change the global dynamics of the structure to improve substructure identification at a particular story. A control law for an active mass damper is developed to increase the interstory response at a particular story, which, when implemented, will improve substructure identification of that story. The control law is developed in simulation and will later be tested experimentally on a four story, 12 ft. steel building excited by base motion.

Keywords Structural Health Monitoring • Structural Control • Structural Dynamics • Damage Detection • Experimental Methods

3.1 Introduction

Following a major earthquake, it is imperative to check buildings for damage. Current practice requires visual inspection to determine if a building is safe, damaged, or unsafe [1]. This practice suffers from three deficiencies. First, visual inspection is costly, requiring teams of trained inspectors. Second, visual inspection is time-intensive because it often takes weeks or months to inspect damaged buildings in an area. Third, visual inspection is inherently subjective and cannot detect damage that is hidden behind partitions and other obstructions.

To overcome the limitations of visual inspections, many researchers have turned their attention to structural health monitoring (SHM). SHM includes automated and data-driven techniques that use measurements of the building response to determine if damage has occurred. Within the class of SHM techniques, several researchers have turned to substructure identification as a way to detect common forms of structural damage. Substructure identification works by identifying a reduced order model of a portion of the structure and detecting damage through stiffness changes. This approach is uniquely beneficial because it reduces the complexity of the analysis model which often makes identification more sensitive to

C. DeVore (✉) • E.A. Johnson
Sonny Astani Department of Civil and Environmental Engineering, University of Southern California,
3620 S Vermont Ave, Los Angeles, CA 90089, USA
e-mail: cdevore@usc.edu; JohnsonE@usc.edu

R.E. Christenson
Department of of Civil and Environmental Engineering, University of Connecticut, 261 Glenbrook Rd., Storrs, CT 06269, USA
e-mail: rchriste@engr.uconn.edu

F.N. Catbas et al. (eds.), *Topics in Dynamics of Civil Structures, Volume 4: Proceedings of the 31st IMAC, A Conference on Structural Dynamics, 2013*, Conference Proceedings of the Society for Experimental Mechanics Series 39, DOI 10.1007/978-1-4614-6555-3_3,

structural damage when compared to global modal methods. In the past two decades, researchers advanced substructure identification through a variety of techniques including an extended Kalman filter (EKF) [2], an auto-regressive moving average with exogenous input (ARMAX) model [3], substructure isolation methods [4], and others.

This study focuses on substructure identification of a shear building in the frequency domain. Zhang and Johnson [5, 6] proposed a method to identify a single story of a shear building by treating it as a single degree of freedom (SDOF) system and using measured accelerations. Within this study, the authors observed that different stories within a uniform shear building exhibit different identification performance. In a follow-up study, Zhang and Johnson [7, 8] proposed using a structural control device to temporarily change the closed-loop dynamics of the structure in a specific way to improve the identification of a particular story.

This paper uses the results of DeVore *et al* [9] to design a feedback controller to improve identification of the second story of an experimental structure. In DeVore *et al* [9], the authors use substructure identification to detect damage in a four story, shear, laboratory-scale experimental building, showing that substructure identification was unable to identify the second story stiffness. Therefore, this paper details the design of a feedback controller to improve substructure identification of the second story.

3.2 Substructure Identification

This section describes the derivation of the substructure identification estimator. First, the reduced order model is described. Second, the estimator is formulated using Newton's second law. Third, the derived estimator is implemented using estimated frequency response functions and least squares estimation. Finally, an approximate error prediction is discussed.

3.2.1 Reduced Order Model

The reduced order model (ROM) used in this study is a shear building model. This model assumes that each floor level can be treated as an independent degree of freedom (DOF) that moves laterally with no rotation. Furthermore, the restoring force provided by the columns is linear in displacement and velocity of the adjacent floor levels. This model is appropriate for civil buildings that have a high beam to column stiffness ratio.

Within the context of substructure identification, the shear building ROM suggests using a single story as the substructure model. Thus, the model function is a SDOF oscillator with transfer function given by

$$H_{\text{MOD}}(s) = \frac{1}{1 + \frac{c_i}{m_i s} + \frac{k_i}{m_i s^2}} \tag{3.1}$$

This model function will be used to estimate the story stiffness and damping parameters (k_i and c_i) of the i^{th} story.

3.2.2 Estimator Formulation

To generate an estimator suitable for the ROM and the selected model function, start with the equation of motion (EOM) for the i^{th} story.

$$m_i \ddot{x}_i + c_i(\dot{x}_i - \dot{x}_{i-1}) + k_i(x_i - x_{i-1}) + c_{i+1}(\dot{x}_i - \dot{x}_{i+1}) + k_{i+1}(x_i - x_{i+1}) = 0 \tag{3.2}$$

Next apply the Laplace transform and various identities to realize $H_{\text{MOD}}(s)$.

$$\frac{1}{1 + \frac{c_i}{m_i s} + \frac{k_i}{m_i s^2}} = \frac{H_{\ddot{x}_i,\ddot{u}_g}(s) - H_{\ddot{x}_{i-1},\ddot{u}_g}(s)}{-H_{\ddot{x}_{i-1},\ddot{u}_g}(s) + [H_{\ddot{x}_{i+1},\ddot{u}_g}(s) - H_{\ddot{x}_i,\ddot{u}_g}(s)]\left(\frac{c_{i+1}}{m_i s} + \frac{k_{i+1}}{m_i s^2}\right)} \tag{3.3}$$

Herein, the right side of (3.3) is referred to as the function of estimated quantities, $H_{\text{EST}}(s)$. This function relates the acceleration response of the i^{th} and adjacent stories to the model function. As such, $H_{\text{EST}}(s)$ will be used to transform

measured acceleration to the model function. It is noted that $H_{\text{EST}}(s)$ requires *a priori* knowledge of the parameters k_{i+1} and c_{i+1} of the story above, which can be provided by a top-down identification where the top story is identified by exploiting free surface boundary conditions. Then, the identified stiffness value is used for identification of the story below and repeated down the height of the structure.

3.2.3 Estimator Implementation

To implement the substructure identification estimator derived in the previous section, an identification functional is created that evaluates the distance between $H_{\text{ROM}}(s)$ and $H_{\text{EST}}(s)$. Thus, for a given value of k_i and c_i, the identification functional is,

$$J = \int |H_{\text{MOD}}(j\omega) - H_{\text{EST}}(j\omega)|^2 d\omega \tag{3.4}$$

Here the integral is evaluated along the imaginary axis as $s = j\omega$. This allows for frequency response functions (FRFs) to be used that are more easily estimated from acceleration records.

In a realistic SHM scenario, the excitation is not measured, which precludes the estimation of input-output FRFs. Instead, $H_{\text{EST}}(j\omega)$ can be formulated to use the interstory FRF, $H_{\ddot{x}_m,\ddot{x}_n}$, with acceleration at the n^{th} floor taken as input and acceleration at the m^{th} floor taken as output. Moreover, by using the acceleration from the identified and adjacent floors ($\ddot{x}_{i-1}$, $\ddot{x}_i$, and $\ddot{x}_{i+1}$), the estimation of $H_{\text{EST}}(j\omega)$ can be decentralized and written three ways. For example,

$$H_{\text{EST}}^{(\ddot{x}_{i-1})}(H_{\ddot{x}_i,\ddot{x}_{i-1}}, H_{\ddot{x}_{i+1},\ddot{x}_{i-1}}, j\omega) = \frac{1 - H_{\ddot{x}_i,\ddot{x}_{i-1}}}{1 + (H_{\ddot{x}_{i+1},\ddot{x}_{i-1}} - H_{\ddot{x}_i,\ddot{x}_{i-1}})\left(\frac{jc_{i+1}}{m_i\omega} + \frac{k_{i+1}}{m_i\omega^2}\right)} \tag{3.5}$$

where $H_{\text{EST}}^{(\ddot{x}_{i-1})}$ is H_{EST} with the floor below, the $(i-1)^{\text{th}}$ floor, chosen as the input signal. By formulating the FRF substructure estimator in three separate ways, the estimator can be designed to use, at each frequency, the most accurate of the three formulas. This is implemented by using as the input, the signal that has the highest power at a particular frequency, which corresponds to a higher signal to noise ratio (SNR).

Finally, with $H_{\text{EST}}(j\omega)$ estimated, k_i and c_i can be estimated using nonlinear least squares estimation. The least squares estimate (LSE) is found by minimizing the sum of the squares error between $H_{\text{MOD}}(j\omega_n)$ and H_{EST}. The sum of the squares error is

$$S(\boldsymbol{\theta}) = \sum_{n=1}^{N} |H_{\text{MOD}}(j\omega_n, \boldsymbol{\theta}) - H_{\text{EST}}(j\omega_n)|^2 \tag{3.6}$$

where $\boldsymbol{\theta} = [k_i, c_i]^{\mathsf{T}}$ is the vector of identified quantities.

3.2.4 Error Prediction

There are certain structure–substructure combinations that lead to poor identification performance as predicted [5] and observed [9]. This study argues that poor identification performance is predicted when there is low magnitude of the interstory acceleration response in the frequency range near interstory natural frequency $\omega_{i,0} = \sqrt{k_i/m_i}$. For the test bed structure (Fig. 3.1a), a pole–zero cancellation is observed at the interstory natural frequency, which, combined with low damping, makes identification of the second story stiffness impossible with substructure identification. This behavior is observed in the frequency response graph in Fig. 3.1b.

3.3 Methods

This section describes the methods used in this study. First, the experimental apparatus is introduced, including the structure, excitation source, and sensors. Next, the the control design procedure is detailed and a feedback controller is designed.

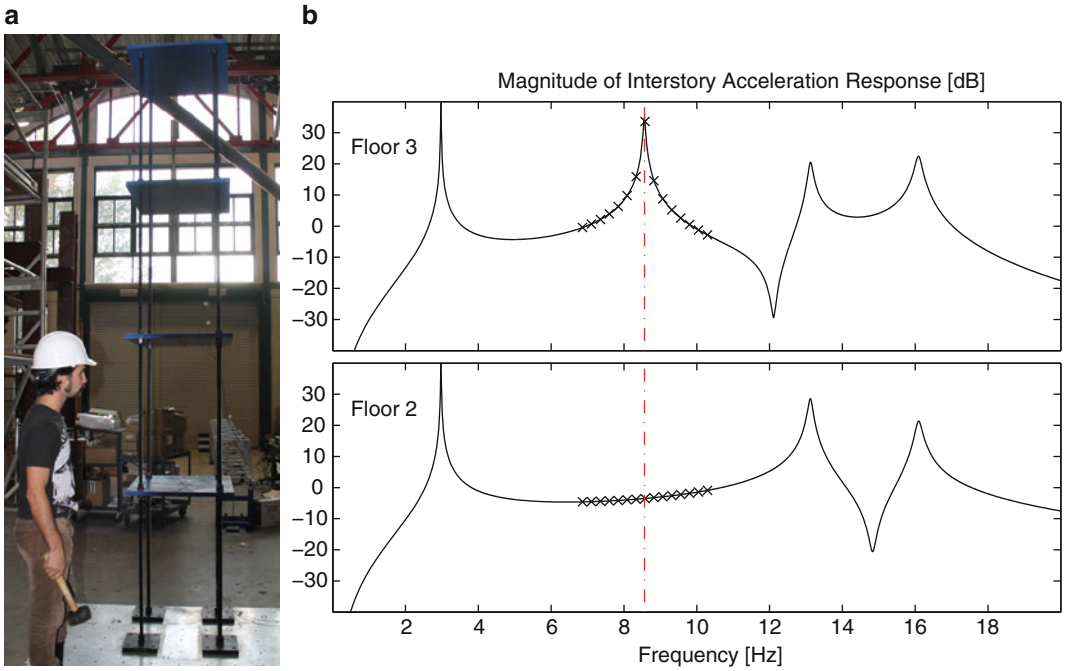

Fig. 3.1 (**a**) Experimental structure and (**b**) plot of interstory acceleration FRF for each story in the structure. *Markers* indicate frequency values that are used in nonlinear regression and the *red dashed line* indicates the maximum response of $H_{\text{MOD}}(j\omega)$. Nominal parameters are used

Table 3.1 Nominal story parameters for four story structure

k_i	126.3 kN/m
c_i	65.3 N/(m/s)
m_i	84.3 kg

3.3.1 Experimental Apparatus

The experimental apparatus is based on a previous experimental study performed at the University of Connecticut [9]. The structure is a four-story, uniform shear building that is symmetric in both plan directions. The building is formed by supporting steel floor plates by four threaded rod columns at the corners. The columns are secured with nuts and lock washers installed above and below each floor plate to ensure the columns behave as fixed-fixed at each story. The nominal parameters for each story level are computed and summarized in Table 3.1.

The excitation source is base motion provided by a 3 ton, uniaxial, 2 m × 2 m shake table. It is run in displacement control and provides a band-limited white noise base excitation. The command signal is pre-filtered such that the shake table achieves a nominally flat acceleration response. The average power of the excitation is characterized by the standard deviation of the table acceleration which is 0.1 m/s^2.

The response of the structure is measured by PCB capacitive accelerometers installed on each floor along the plan centerline in the direction of excitation. The accelerometers are sampled at 256 Hz for 512 seconds for each trial. A noise analysis is performed and the accelerometers are found to have SNR of 30 dB.

3.3.2 Control Design

To improve the identification performance of the second story stiffness parameter, a feedback controller for an active mass driver (AMD) is designed consistent with the error analysis described in Section 3.2.4 and [7]. The AMD is installed on the top floor of the structure and it is assumed that the AMD is able to apply a perfect force command. This assumption is unrealistic but control design can be later extended to use an experimentally-derived transfer function from AMD command

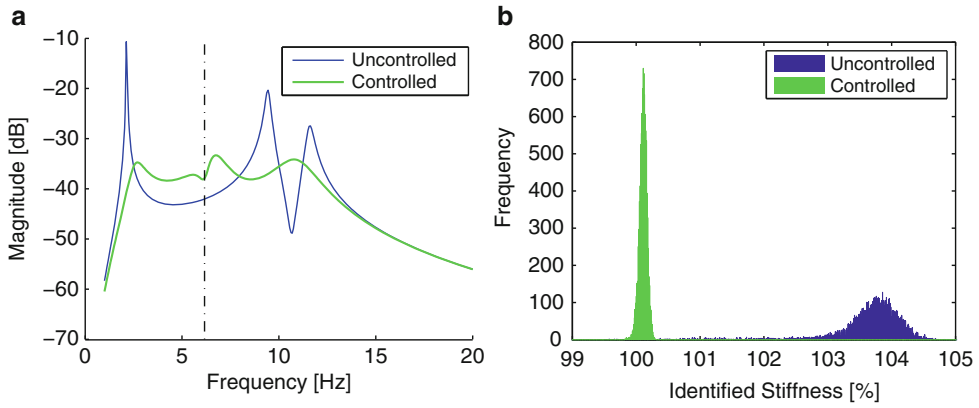

Fig. 3.2 (**a**) Second story interstory acceleration frequency response with and without control. The interstory natural frequency is marked by a *dashed line*. (**b**) Histogram of identified second story stiffness values expressed as a percentage of the nominal stiffness. The total number of samples is 10,000 with 876 outliers for the uncontrolled system and 78 outliers with controlled system. Outliers are defined as identification results outside the range of (99%, 105%)

to AMD force or, more generally, structural response. A shear building model is used with the nominal parameters found in the previous section, which was found to have good agreement with experimental values [9]. In this study, it is assumed that perfect state estimation is available and, therefore, closed-loop poles $\mathbf{p}$ are used as the search space for control design. This innovation allows specifying the closed-loop poles and finding a feedback gain $\mathbf{K}(\mathbf{p})$ using pole placement. As such, the controller is found by minimizing the functional

$$\arg\max_{\mathbf{p}} \int_{0.8\omega_0}^{1.2\omega_0} \left| W(j\omega)\, H^{\mathbf{K}(\mathbf{p})}_{\ddot{x}_i - \ddot{x}_{i-1}, \ddot{u}_g}(j\omega) \right|^2 d\omega \tag{3.7}$$

where $H^{\mathbf{K}(\mathbf{p})}_{\ddot{x}_i - \ddot{x}_{i-1}, \ddot{u}_g}$ is the closed-loop interstory acceleration frequency response function for the i^{th} story given closed-loop poles $\mathbf{p}$ and $W(j\omega)$ is a weighting function that assumes the shape of a SDOF oscillator. The minimization is subject to the constraints that the real component of the closed loop poles are less than the largest real component of the uncontrolled poles and that the damping of the closed loop system be larger than 10% in each mode (*i.e.*, Re $p_i < -0.1|p_i|$). An additional constraint that the force applied be less than 100 N is used but is found to be an inactive constraint as the force levels were significantly smaller. Numerical optimization is provided by the MATLAB® command `fmincon` using an interior-point algorithm.

The damping constraint was found to have a significant effect on the controller design by limiting the maximum response below −30 dB. Likewise, the control functional had the effect of placing two poles near the interstory natural frequency (6.16 Hz). The effect of the controller on the second story interstory acceleration response is shown in Fig. 3.2a.

3.4 Results

To verify the improved identification performance of controlled substructure identification, Monte Carlo simulation is used. Acceleration time histories are generated and then analyzed using the substructure identification methods described in Section 3.2.3 to find the second story stiffness parameter. The stiffness parameter is recorded and the process is repeated 10,000 times for both the uncontrolled and controlled systems.

The results of Monte Carlo simulation are summarized by the statistics in Table 3.2 and the histogram in Fig. 3.2b. Gaussian sample statistics (mean and standard deviation) are reported with robust statistics (median and inter-quartile range (IQR)) because, while the identified stiffness parameter converges to a Gaussian distribution, there are significant outliers. By direct comparison of the statistics and visual inspection of the histogram, it is evident that the controlled system exhibits increased accuracy and decreased variance, whereas the uncontrolled identification has significant bias as well as large deviations.

Table 3.2 Identification statistics for second story stiffness with and without control expressed as a percentage of the nominal value

	Mean	St. dev.	Median	IQR
Uncontrolled	107.12	13.43	103.79	0.53
Controlled	99.72	4.41	100.11	0.08

3.5 Conclusions

The results indicate that the identification accuracy and precision of the second story stiffness is much greater using the designed feedback controller. Further, there are fewer trials for which identification fails, evidenced by a decreased number of outliers (876 decreased to 78). While the controller enables superior identification performance, it relies on full state estimation which will not be available in a laboratory setting. Prior to implementation in experiment, it is necessary to design and simulate the effects of a state observer on identification performance. Experimental verification is planned using the developed feedback controller.

References

1. ATC (1989) ATC-20: procedures for postearthquake safety evaluation of buildings, Tech. Rep. Applied Technology Council, Redwood City
2. Koh CG, See LM, Balendra T (1991) Estimation of structural parameters in time domain: a substructure approach. Earthquake Eng Struct Dynam 20(8):787–801
3. Xing Z, Mita A (2012) A substructure approach to local damage detection of shear structure. Struct Contr Health Monit 19(2):309–318
4. Hou J, Jankowski Ł, Ou J (2011) A substructure isolation method for local structural health monitoring. Struct Contr Health Monit 18(6): 601–618
5. Zhang D, Johnson EA (2013) Substructure identification for shear structures I: substructure identification method. Struct Contr Health Monit 20(5):804–820
6. Zhang D, Johnson EA (2006) Substructure parameter identification method for shear type structures. In: Proceedings of 4th world conference on structural control and monitoring, San Diego, CA, 2006
7. Zhang D, Johnson EA (2013) Substructure identification for shear structures II: controlled substructure identification. Struct Contr Health Monit 20(5):821–834
8. Zhang D, Johnson EA (2006) Controlled substructure identification method for shear type structure. In: Proceedings of 4th world conference on structural control and monitoring 2, San Diego, CA, 2006
9. DeVore C, Jiang Z, Johnson EA, Christenson RE, Stromquist-Levoir G (2012) Experimental verification of substructure identification for damage detection. In: Proceedings of the 2012 engineering mechanics institute conference, South Bend, IN, 2012